https://doi.org/10.5194/essd-2026-153
Preprint. Discussion started: 22 June 2026

Open Access Earth System Science Data Discussions

A review of Last Interglacial sea-level proxies in South Asia and the Indian Ocean

Mubashir Ali[1], Ciro Cerrone[1,2], Alessio Rovere[1,3*]

[1]Department for Environmental Sciences, Informatics and Statistics (DAIS), Ca' Foscari University of Venice, Via Torino 155, Venice, 30172, Italy
[2]International Centre for Climate Change Research and Studies (CSRCC), Franchetti Palace, San Marco 2847, 30124 Venice, Italy
[3]MARUM, Center for Marine Environmental Sciences, University of Bremen, Leobener Str. 8, 28359 Bremen, Germany

Correspondence to: Alessio Rovere (alessio.rovere@unive.it)

Abstract. In this work, we present a standardized database of Last Interglacial (132-80 ka) sea-level proxies across the South Asian and Indian Ocean region, including the coasts of Iran, Oman, India, the Maldives, and the Cocos (Keeling) Islands. The database stems from a critical revision of the data included in 17 peer-reviewed studies, which were standardized using the World Atlas of Last Interglacial Shorelines (WALIS), and is available as Ali et al. (2026, https://doi.org/10.5281/zenodo.18512770). A total of 54 sea-level index points were reassessed by evaluating stratigraphic context, elevation measurement techniques, depositional environments, and chronological constraints obtained from U-series, luminescence, electron spin resonance, and cosmogenic nuclide dating. The data is characterized by regional differences in the elevation of past relative sea-level proxies that are driven primarily by tectonic, dynamic topography, and glacio-hydro-isostatic forcings. On the active margins of southern Iran and northern Oman, terraces dated to Marine Isotopic Stage (MIS) 5e (125 ka), 5c (100 ka), and 5a (80 ka) were preserved at 20–60 m a.s.l., reflecting long-term uplift linked to the Zagros foreland and Makran subduction system. On the coasts of western and southern India MIS 5e relative sea-level proxies are found at 1-4 m a.s.l., more in line with low tectonic uplift. On Indian Ocean islands, such as the Maldives and Cocos (Keeling) Islands, MIS 5e reefs are now submerged at depths of 10-17 m b.s.l., indicating subsidence throughout the late Quaternary.

1 Introduction

This study reviews evidence of relative sea-level (RSL) proxies from the Last Interglacial (LIG), broadly corresponding to the Marine Isotope Stage (MIS) 5 (132-80 ka), across the South Asia Indian Ocean region, including the Maldives, India, Oman, and the southern coasts of Iran (Fig.1). Pakistan has not been incorporated into the database due to the limited availability of published metadata, which has prevented the standardization of sea-level data for this region. The database was assembled by extracting and re-analysing data and metadata from peer-reviewed publications that provide stratigraphic records and chronological information related to Quaternary sea-level variations in the region. Data on sea-level indicators and associated chronological information were standardized through the use of the World Atlas of Last Interglacial Shorelines (WALIS) platform (Garzón and Rovere, 2024; Rovere et al.,

https://doi.org/10.5194/essd-2026-153
Preprint. Discussion started: 22 June 2026

Open Access Earth System Science Data Discussions

2020, available at: https://warmcoasts.eu/world-atlas). The database was exported from the WALIS interface in spreadsheet format and is available as an Excel file via Zenodo under a CC-BY license (Ali et al., 2026, https://doi.org/10.5281/zenodo.18512770). Table 2 included in the text, provides a summary of the elevation, chronological constraints, references, and quality assessments for each RSL data point included in the investigated area.

This study focuses on a region that helps fill existing geographic gaps in previous global compilations of sea-level indicators related to LIG (Rovere et al., 2023) and serves as an update and extension to earlier datasets, such as that presented by Pedoja et al., 2014. Regionally, this work integrates a recent compilation (also done in the framework of WALIS) along the East Africa and the Western Indian Ocean was compiled by Boyden et al. (2021). Altogether, data from 17 peer-reviewed studies were compiled, yielding 54 relative sea level index points (SLIPs). The database compilation was finalized in September 2025; accordingly, data from papers published after this date were not included. Each SLIP was assigned one or more chronological constraints. In particular, we inserted in the database data and metadata related to samples dated with luminescence (n = 7), U-series (n = 20 on corals, n = 4 on mollusks), electron spin resonance (ESR; n = 22), and one cosmogenic radionuclide (^{10}Be) techniques.

A brief description of the types of sea-level indicators within this study is provided in the following section. This is followed by a discussion of elevation measurement methods, sea-level reference datums, and main dating techniques used by the original authors. Finally, the data points are described and organized according to national and regional boundaries.

https://doi.org/10.5194/essd-2026-153
Preprint. Discussion started: 22 June 2026

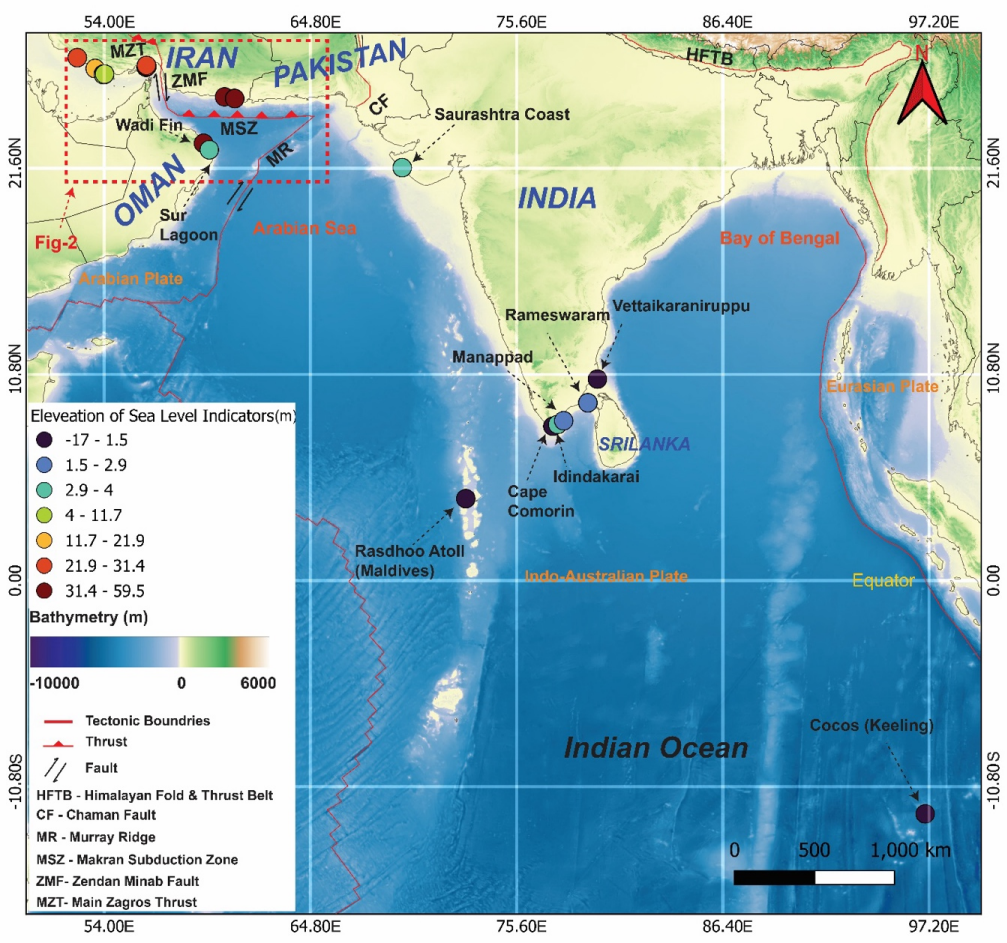

Figure 1 Sea Level Index Points (SLIPs) revised in South Asia and the Indian Ocean region. Colored dots show sea-level datapoints included in the WALIS database, with colors indicating elevation. Red lines represent tectonic plate boundaries from Bird (2003), modified by H. Ahlenius (Nordpil, GitHub: https://github.com/fraxen/tectonicplates). Basemap assembled from datasets provided by the Global Multi-Resolution Topography (GMRT) (Ryan et al., 2009).

2 Types of sea-level indicators, positioning and sea-level datums

Seven main types of SLIPs were identified in our study area (Table 1). These include three depositional (beach deposit or beachrock, beach ridge, beachrock), two biological (coral reef terrace, shallow or intertidal marine fauna) and two geomorphological indicators (marine terrace and tidal notch). To establish a connection between these indicators and past relative sea levels, we employed the concept of indicative meaning, a methodological framework that quantifies how specific sea-level markers relate to tidal datums (Khan et al., 2019). This framework defines that each indicator must be assigned an indicative meaning, which is decomposed into two values: the indicative range (IR), which

https://doi.org/10.5194/essd-2026-153
Preprint. Discussion started: 22 June 2026

captures the vertical range at which a SLIP can occur according to its modern analog (Khan et al., 2019), and the reference water level (RWL), that is the midpoint of the IR. Originally developed for Holocene studies (Shennan, 1982, 1986, 1989; Shennan et al., 1983; Shennan, 2015), the indicative meaning approach has more recently been applied to Pleistocene sea-level proxies (Rovere et al., 2016b), allowing for consistent interpretation of SLIPs across different time periods. To quantify the indicative meaning, here we used the IMCalc software (Lorscheid and Rovere, 2019), which generates ex situ estimates of RWL and IR using global tidal and wave datasets. This approach is particularly useful when a direct, site-specific modern analogue data from primary sources are not available, as it is the case for the works published in our study area.

While elevation measurement techniques are reported in most of the studies included in our review, a limited number in Iran do not provide this information (Reyss et al., 1998; Normand et al., 2019). In instances where the method of elevation measurement was not reported, we applied an estimated error of 20% of the reported elevation to account for potential inaccuracies (Rovere et al., 2016b). Among the six measurement techniques recorded in this database, the vast majority of sea-level index point elevations were determined using barometric altimeters and tape and Abney (a handheld surveying instrument used to measure slope angles, gradients, and vertical heights) levelling. Other elevation measurement techniques include (i) differential GPS in the Sur lagoon area (Oman, Mauz et al., 2015a; Falkenroth et al., 2020), offering the highest measurement accuracy; (ii) a combination of differential GPS, hand level, and tape in Oman (Hoffmann et al., 2020; Decker et al., 2024; Falkenroth et al., 2019); and (iii) handheld GPS in Iran and Maldives (Pirazzoli et al., 2004; Gischler et al., 2008a,b; Gischler et al., 2018a,b; Normand et al., 2019; Goswami et al.,2019). A couple of works (Brückner, 1989; Goswami et al., 2019) do not report any elevation measurement technique for the (i) Porbandar and Tunkra and (ii) Tamil Nadu areas, respectively. Since most studies did not report exact site coordinates, we estimated them using place names via geolocation tools (e.g., Google Maps) or by georeferencing original maps in QGIS.

Table 1 Summary of sea-level proxies included in the South Asian and Indian Ocean database. Abbreviations: MLLW - Mean Lower Low Water; MHHW - Mean Higher High Water; HAT - Highest Astronomical Tide.

SLIP	Description of RSL indicator	Indicative range	Indicator reference(s)	Number of occurrences in the database
Beach deposit or beachrock	Definition by Mauz et al., 2015: "Beachrocks are lithified coastal deposits that are organized in sequences of slabs with seaward inclination generally between 5° and 15°".	Ordinary berm to breaking depth	Mauz et al., 2015a; Rovere et al., 2016b	3
Beach ridge	Definition by Otvos, 2000: "[beach ridges are] stabilized, relict intertidal and supratidal, eolian and wave-built shore ridges that may consist of either siliciclastic or calcareous clastic matter of a wide range of clasts dimensions, from fine sand to cobbles and boulders".	Storm wave swash height to ordinary berm	Otvos, 2000; Rovere et al., 2016b	1
Beachrock	Cement: isopachous or miniscus of HMC or aragonite; granular, bladed or fibrous crystals Bedding: symmetrical ripples or horizontal plane-parallel laminae or planar and trough cross-beds	HAT (or spray zone) to MLLW	Mauz et al., 2015b	2
Coral reef terrace (general definition)	Coral-built flat surface, corresponding to shallow-water reef terrace to reef crest.	MLLW to breaking depth	Rovere et al., 2016b;	32

https://doi.org/10.5194/essd-2026-153
Preprint. Discussion started: 22 June 2026

			Lorscheid and Rovere, 2019	
Marine Terrace	Definition by Pirazzoli et al., 2005: "Any relatively flat surface of marine origin".	Storm wave swash height to breaking depth	Pirazzoli, 2005; Rovere et al., 2016b	10
Shallow or intertidal marine fauna	Marine fauna usually associated with very shallow water or intertidal environments	Based on the upper and lower limits of living modern analog faunas		5
Tidal notch	Definition by Antonioli et al., 2015: "Indentations or undercuttings cut into rocky coasts by processes acting in the tidal zone (such as tidal wetting and drying cycles, bioerosion, or mechanical action)".	MHHW to MLLW	(Antonioli et al., 2015); Rovere et al., 2016b	1

3 Relative sea-level data

In the following sections we describe the data we revised, organized by country in a clockwise order starting from Iran, and, where applicable, by subordinate administrative units such as states, regions, or provinces. Throughout the text, the elevation of SLIPs is expressed as “a.s.l.” (above present sea level) or “b.s.l.” (below present sea level). A summary of sites, associated paleo RSL, and chronological constraints associated to each site are detailed in Table 2. Sea-level indicators compiled in the database are referenced by their WALIS RSL ID (hereafter RSL_NUMBER). This identifier, displayed in the first column of the “RSL proxies” spreadsheet, is automatically generated and uniquely assigned to each record within WALIS.

Table 2 Summary of SLIPs and dated samples / chronostratigraphic constraints for the South Asia and Indian Ocean region. Legend for SLIP types: CRT = Coral Reef Terrace; MT = Marine Terrace; BD = Beach deposit or beachrock; SIMF = Shallow or intertidal marine fauna; TN = Tidal notch; and BR = Beach Ridge.

Walis ID	Site Name	Latitude	Longitude	SLIP Type	Elevation (m)	Paleo RSL (m)	MIS	Age (ka)	Orginal dating ID	References
RSL_4527	Haleh	27.396944	52.593889	CRT	23±5	23.63±5	MIS5e/MIS5c	111±4	HA7	Reyss et al., 1998
RSL_4528	Jazeh	26.826667	53.528056	MT	9±5	8.77±5	MIs5e	130±13	JA8	
RSL_4529	Jazeh	26.826667	53.528056	MT	21±5	20.76±5	MIS5e	118±10	JA9	
RSL_4507	Kish Island	26.535278	54.025556	CRT	5.2±2	5.89±2	MIS5e	126±14	0KI-08	Pirazzoli et al., 2004 Preusser et al., 2003
RSL_4508	Kish Island	26.535278	54.025556	CRT	6.7±2	7.39±2	MIS5e	122±10	0KI-10	
RSL_4509	Kish Island	26.535278	54.025556	CRT	8.1±2	8.79±2	MIS5e	117±18	0KI-11	
RSL_4510	Kish Island	26.535278	54.025556	CRT	11.6±2	12.29±2	MIS5e/MIS5c	100±9	0KI-14	
RSL_4511	Kish Island	26.506111	53.999444	CRT	18±2	18.69±2	MIS5e/MIS5d	115±15	0KI-15	
RSL_4512	Kish Island	26.506111	53.999444	CRT	18±2	18.69±2	MIS5e	126±12	0KI-16	
RSL_4513	Kish Island	26.506111	53.999444	CRT	18±2	18.69±2	MIS5e/MIS5d	114±16	0KI-17	
RSL_4514	Kish Island	26.536389	53.958889	CRT	32±1	32.69±1	MIS5	148±20	0KI-23	
RSL_4515	Kish Island	26.536389	53.958889	CRT	32±1	32.69±1	MIS5e	128.5±4	OKI-24	
RSL_4515	Kish Island	26.536389	53.958889	CRT	32±1	32.69±1	MIS5e	119±10	0KI-24	
RSL_4516	Kish Island	26.499167	53.966944	CRT	6±2	6.69±2	MIS5e	116±33	OKI-03	
RSL_4516	Kish Island	26.535278	54.025556	CRT	6±2	6.69±2	MIS5e	248±15	0KI-03	
RSL_4536	RSL_4536	26.535278	54.025556	CRT	8.4±2	9.08±2	MIS5e	143±12	OKI-12	
RSL_4517	Qesham	26.926111	56.211111	CRT	3±2	3.79±2	MIS 5e	133±10	0QE-29	Pirazzoli et al., 2004
RSL_4518	Qesham	26.926111	56.211111	CRT	12±5	12.79±5	MIS5	139±6	QE100	Reyss et al., 1998 Pirazzoli et al., 2004
RSL_4519	Qesham	26.991667	56.217222	CRT	20±1	20.8±1	MIS 5e	133±13	0QE-51	Pirazzoli et al., 2004
RSL_4520	Qesham	26.990556	56.216667	CRT	21±5	21.8±5	MIS 5e	127±6	QE102	Reyss et al., 1998 Pirazzoli et al., 2004
RSL_4521	Qesham	26.928056	56.216944	CRT	26±2	26.79±2	MIS 5e	126±11	0QE-40	Pirazzoli et al., 2004
RSL_4522	Qesham	26.893333	56.197778	CRT	26±5	26.78±5	MIS5c	104±5	QE54	Reyss et al., 1998 Pirazzoli et al., 2004
RSL_4523	Qesham	26.929444	56.238056	CRT	30±2	30.79±2	MIS 5e	123±18	0QE-33	Pirazzoli et al., 2004
RSL_4524	Qesham	26.991667	56.217222	CRT	30±2	30.8±2	MIS 5e	115±9	0QE-53	
RSL_4525	Qesham	26.929444	56.238056	CRT	30±2	30.79±2	MIS 5e	137±11	0QE-34	
RSL_4526	Qesham	26.991667	56.217222	CRT	25±2	25.8±2	MIS 5e	138±12	0QE-52	
RSL_4532	Konarak T3	25.343285	60.305565	MT	32.3±2	31.76±2.7	MIS 5e	141.3±12	RN17-48	Normand et al., 2019
RSL_4531	Ramin T1	25.261995	60.827053	MT	59.5±2	58.93±2.8	MIS 5e	140.21±12	RN17-43	
RSL_4530	Lipar T3	25.249691	60.841739	MT	58.5±2	57.93±2.8	MIS 5e	130.28±10	RN17-30	
RSL_4501	Oman (Terrace T3)	22.911695	59.205471	BD	36.7±1	36.44±1.3	MIS5	97±6	DEL4-Q	Hoffmann et al.,2020 Decker et al.,2024 Falkenroth et al., 2019
RSL_4501	Oman (Terrace T3)	22.911695	59.205471	BD	36.7±1	36.44±1.3	MIS5	118±8	DEL5-Q	
RSL_4502	Sur Lagoon	22.5821	59.4518	TN	3.93±0.12	4.04±0.94	MIS5	< 371 >80	TD13-009	Falkenroth et al., 2020

RSL_4541	Sur Lagoon	22.567297	59.507797	BD	3.73	3.76±1.3	MIS5	80±3	LV565	Mauz et al., 2015a
RSL_4540	SAURASHTRA COAST	21.634782	69.610289	SIMF	4	5.53±0.4	MIS5	95	Por 1c-M /1:1	Brückner, 1989
RSL_4540	SAURASHTRA COAST	21.634782	69.610289	SIMF	4	5.53±04	MIS5	97.6±10	Tun 2d (D-1292)	
RSL_4540	SAURASHTRA COAST	21.634782	69.610289	SIMF	4	5.53±0.4	MIS5	94.9±10	Por 1c-S (D-1278)	
RSL_4540	SAURASHTRA COAST	21.634782	69.610289	SIMF	4	5.53±0.4	MIS5	105±10	Por 1b (D-1277)	
RSL_4492	Cape Comorin	8.085205	77.496911	BD	1.2±0.5	1.53±1.7	MIS5e/5c	112±10	Cape C	Banerjee, 2000 Brückner, 1989
RSL_4493	Idindakarai	8.182555	77.755555	SIMF	3.4±0.5	3.38±5	MIS 5e	124±11	Vija52	
RSL_4494	Manappad	8.373333	78.066666	BD	2.5±0.5	2.44±1.6	MIS 5e	120±8	Tuti 2b	
RSL_4489	Rameswaram	9.313888	79.333333	CRT	1.1±0.5	1.83±0.7	MIS 5e	125.6±8	PKB 8a	Banerjee, 2000
RSL_4490	Rameswaram	9.313888	79.333333	CRT	2.9±0.5	3.63±0.7	MIS5c	104±10	R5	
RSL_4491	Rameswaram	9.313888	79.333333	CRT	2.9±0.5	3.63±0.7	MIS 5e	116±10	R3	
RSL_4503	Rameswaram	9.313888	79.333333	CRT	2.9±0.5	3.63±0.7	MIS5c	92±6	R6	
RSL_4504	Rameswaram	9.313888	79.333333	CRT	2.4±0.5	3.13±0.7	MIS5e/MIS5d	112±8	Vadakadu4	Banerjee et al., 2000 Brückner, 1989
RSL_4504	Rameswaram	9.313888	79.333333	CRT	2.4±0.5	3.13±0.7	MIS 5e	139±10	Vadakadu 4	
RSL_4505	Rameswaram	9.313888	79.333333	CRT	2.9±0.5	3.63±0.7	MIS5c	104±10	R7	Banerjee, 2000
RSL_4506	Rameswaram	9.313888	79.333333	CRT	2.4±0.5	3.13±0.7	MIS5c	108±3	01/97	
RSL_4539	Vettaikaraniruppu	10.553467	79.83545	BR	-13.5	12.59±0.2	MIS 5e	121±11	VKI12F	Goswami et al.,2019
RSL_4495	Rasdhoo Atoll	4.291922	72.940327	CRT	-15.2	-14.18±0.6	MIS5e	136.9±2	1-14.2	Gischler et al., 2008a,b Gischler et al., 2018a
RSL_4537	Rasdhoo Atoll	4.291922	72.940327	CRT	-16.3	-15.27±0.6	MIS5e	114.3±2	1-15.3	
RSL_4538	Rasdhoo Atoll	4.291922	72.940327	CRT	-17	-15.97±0.6	MIS5e	117.3±3	1-16.0	
RSL_4496	Keeling	-12.222222	96.999999	CRT	-10.5±1	-9.19±1	MIS5e	123±7	sample without cement	Woodroffe et al., 1991 Woodroffe, 2005
RSL_4496	Keeling	-12.222222	96.999999	CRT	-10.5±1	-9.19±1	MIS5e	118±7	Bulk sample	

https://doi.org/10.5194/essd-2026-153
Preprint. Discussion started: 22 June 2026

Open Access Earth System Science Data Discussions

3.1 Iran

3.1.1 Southern Mainland Iran

The Northern margin of the Persian Gulf in southern Iran hosts a broad coastal sector that provides important archives for Quaternary sea-level reconstructions (Fig. 2). The Haleh coastal sector (Fig. 1B), situated along the southern Iranian mainland, comprises a series of stepped marine terraces that record past sea-level fluctuations over the Quaternary (e.g., Reyss et al., 1998). Similarly, the Jazeh coastal area (Fig. 2) preserves a well-defined sequence of Quaternary marine terraces, offering an additional, complementary record for reconstructing relative sea-level evolution in the region (Reyss et al., 1998). Moving eastward, the Konarak, Ramin, and Lipar areas, along the southern coastal margin of Iran (Fig. 2), also host late Quaternary RSL indicators (e.g., Normand et al., 2019). Together, these coastal sites provide critical datasets for understanding the timing, magnitude, and variability of past sea-level changes along this tectonically active margin.

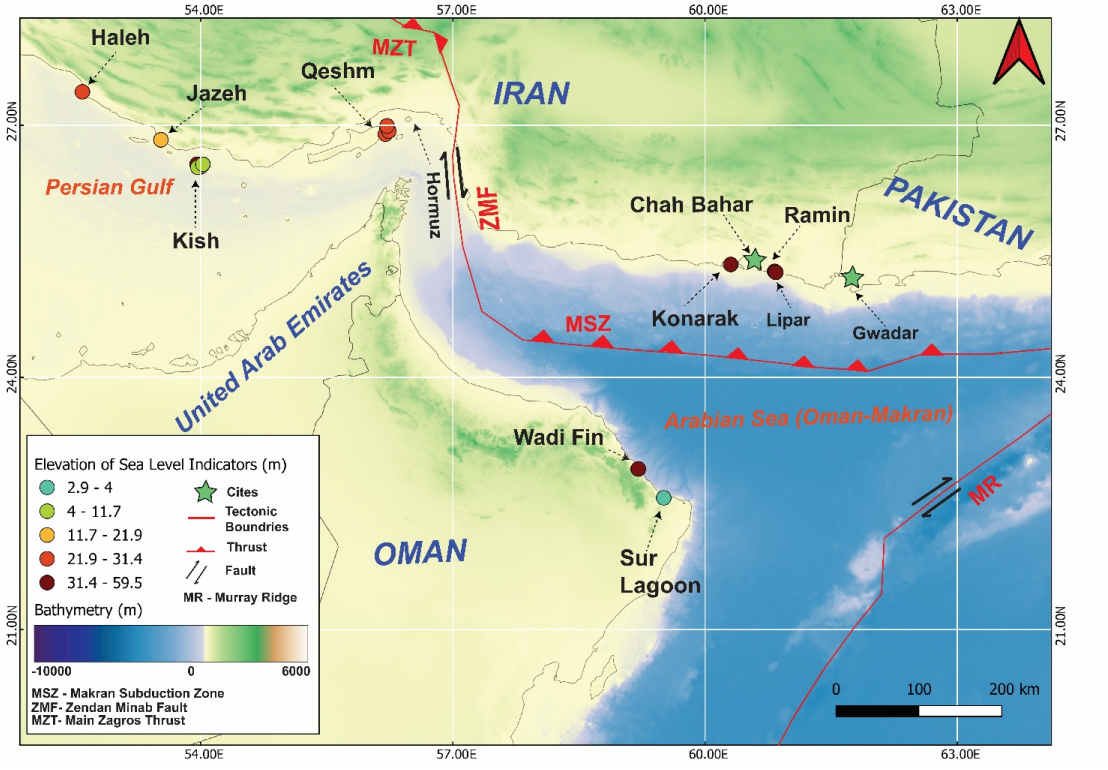

Figure 2 Map of the southern coast of Iran and northern Oman, showing the locations of SLIPs from this region. Basemap assembled from datasets provided by the Global Multi-Resolution Topography (GMRT).

https://doi.org/10.5194/essd-2026-153
Preprint. Discussion started: 22 June 2026

3.1.1.1 Haleh

Along the Haleh coastal sector, a staircase of well-preserved marine terraces is exposed, reaching elevations exceeding 100 m a.s.l. (Reyss et al., 1998). The terrace sequence includes a highly elevated coral-bearing unit at 100–110 m a.s.l., a narrower abrasion terrace at 85 m a.s.l., and a broad reef platform that gently slopes from 33 to 23 m a.s.l., before merging seaward into a low, cliffed bench situated between 5 and 2.5 m a.s.l. Among these three orders, the third terrace (33–23 m) is particularly well constrained in terms of its elevation, morphology, stratigraphic context and age. Near the seaward edge of this terrace, which represents a previous reef platform, coral colonies preserved in growth position have been sampled and dated using U-series techniques, yielding an age of 111 ± 4 ka (Reyss et al., 1998). This age corresponds to MIS 5e or MIS 5c and has been included in WALIS as RSL_4527. The lithofacies assemblages are typical of shallow-marine reef-flats environments, including coral framestones interbedded with lumachelle-bearing limestones and bioclastic sands, which rest unconformably over Mio-Pliocene marls.

3.1.1.2 Jazeh

Three major terrace orders are exposed along the coastal area of Jazeh (Fig.2): (i) a higher surface at 60–65 m, (ii) a broad intermediate terrace sloping between 35 and 25 m, and (iii) a narrow low bench near the modern shoreline recorded by Reyss et al. (1998). The Last Interglacial RSL indicators are preserved within the intermediate terrace, where *in situ Porites* corals were sampled and dated by U-series techniques. Two of these *in situ* corals yielded U-series ages of 121 ± 6 ka and 117 ± 6 ka (WALIS IDs RSL_4528 and RSL_4529, respectively), consistent with deposition during MIS 5e. The dated corals are associated with framestone lithofacies interbedded with lumachelle-rich limestones and bioclastic sands, suggesting shallow reef-flat to nearshore depositional environments.

3.1.1.3 Koranak

The Konarak T3 terrace, located on the southeastern Makran coastline (Fig. 2), is characterized by flat-topped, bedrock deposits interbedded with various-sized boulders. In WALIS, this terrace is catalogued as RSL_4532, with a shoreline angle elevation at 32 m a.s.l. Optically stimulated luminescence (OSL) dating of feldspar from the terrace T3 yielded a fading-corrected age of 141.3 ± 12.1 ka, which falls within the broader range of MIS 5e (Normand et al., 2019). However, the combined morphological expression, facies, and chronological evidence provide strong grounds for assigning T3 to the Last Interglacial highstand. The Konarak T3 terrace, however, is substantially higher than global eustatic benchmarks for MIS 5e, which are generally constrained to 6 to 9 m a.s.l. (Hearty et al., 2007; Dutton & Lambeck, 2012). The calculated uplift rate for this lies therefore between 0.15–0.25 mm/yr (Normand et al., 2019)

3.1.1.4 Ramin

The Ramin coastal site, situated east of Chabahar on the Makran margin (Fig. 2), features a prominent marine terrace (T1) preserved at an elevation of 59.5 ± 2.0 m a.s.l., recorded in the WALIS database as RSL_4531. This terrace T1 is composed of trough-cross stratified bedrock deposits. Luminescence dating of sediments associated to T1 marine

https://doi.org/10.5194/essd-2026-153
Preprint. Discussion started: 22 June 2026

terrace yielded an age of 140.2 ± 12.5 ka, which corresponds to MIS 5e interval (Normand et al., 2019). However, the lower part of Ramin T1 at 3 m of elevation is dated with OSL, which provides the age 78 ka and interprets T1 as MIS 5a (Normand et al., 2019; Thompson & Creveling, 2021). The WALIS record (RSL_4531) and the geomorphic, chronological, and stratigraphic evidence at Ramin T1 together support its use as a significant but tectonically displaced RSL indicator of Last Interglacial.

3.1.1.5 Lipar

The Lipar coastal plain, located along the eastern Makran margin of southeastern Iran, holds the Late Quaternary isolated, flat-topped, marine terrace deposits of beachrocks in the Persian Gulf Arabian Sea region (Fig. 2). Three main terrace orders have been described at this site by Normand et al. (2019). The lowest two (T1 and T2) occur between 20 and 50 m a.s.l. and consist of beachrock deposits interbedded with various-size boulders and shell fragments. The sedimentary structures are dominated by high to low-angle trough cross-stratification, which shows that the deposition of Lipar T1 and T2 deposits occurs in high-energy marine environments. OSL dating provides the age constraints for T1 and T2, yielding ages between 73 and 80 ka and correlating them with MIS 5a (Normand et al., 2019; Thompson & Creveling, 2021). Further inland and higher on the coastal slope, the most prominent surface is the Lipar T3 terrace, occurring up to 58.5 m a.s.l. The lithological composition is similar to that of Lipar T1 and T2, and is mainly composed of beach rock deposits interbedded with various-sized boulders and shell fragments. The sedimentary structures include high to low-angle trough cross stratification, which characterizes the deposition of Lipar T3 and indicates a high-energy marine environment. The OSL-based chronology yielded an age of 130.28 ± 10 ka, corresponding to MIS5e. Consistent ages make it one of the clearest RSL indicators of the Last Interglacial highstand along the Makran coast, archived in the WALIS database as RSL_4530. The elevations of both MIS 5e (T3) and MIS 5a (T1–T2) terraces are significantly higher than global eustatic estimates, which place MIS 5e at 6 to 9 m a.s.l. (Hearty et al., 2007; Dutton & Lambeck, 2012) and MIS 5a generally below +6 m (Thompson & Creveling, 2021). The calculated long-term uplift rates of approximately 0.15–0.25 mm/yr for Lipar are based on the combined elevation and ages of these terraces (Normand et al., 2019).

3.1.2 Iran's islands

Most of the late Quaternary RSL indicators reported in the literature for the southern coast of Iran originate from its islands, including Kish and Qeshm islands, which are in the vicinity of the Hormuz Strait (Fig. 2). A brief description of these areas is provided below.

3.1.2.1 Kish Island

Kish Island, situated in the southeastern Persian Gulf about 20 km off the Iranian mainland, preserves a staircase of raised coral reef terraces that represents one of the best-documented records of Last Interglacial (MIS 5) sea-level change in the region. Kish Island, rising to c. 32 m a.s.l., is composed predominantly of Pleistocene reef limestones that have been systematically mapped and chronologically studied by several studies (Preusser et al., 2003; Pirazzoli

https://doi.org/10.5194/essd-2026-153
Preprint. Discussion started: 22 June 2026

et al., 2004). The most reliable Last Interglacial indicators are reef terraces occurring between 5 and 12 m a.s.l. (RSL_4507, RSL_4508, RSL_4509, RSL_4510, RSL_4516, and RSL_4536). These terraces are composed of coral framestones and boundstones dominated by *Platygyra*, *Favia*, *Porites*, and *Goniastrea*. These coral colonies are preserved in growth position and are overlain by reef debris and cemented bioclastic sands. Such lithofacies are characteristic of shallow subtidal to intertidal reef accretion during stable highstands. Chronological constraints are primarily based on ESR and U-series dating of corals. The ESR results consistently fall between 100 and 126 ka, with most values clustering at 122–126 ka, consistent with deposition during the Last Interglacial highstand (Preusser et al., 2003). At an elevation of 6 m a.s.l., one U-series date yielded an anomalous age of 248 ± 15 ka, likely due to reworked material from higher (and older) terraces. However, the same sample produced an ESR age of 116 ± 33 ka, which is consistent with deposition during MIS 5e (Pirazzoli et al., 2004).

The coral reef terraces occurring between 18 and 32 m a.s.l. (WALIS IDs 4511–4515) yielded ESR and U-series ages in the range of 114–126 ka, again strongly corresponding to MIS 5e. However, their anomalously high position relative to global eustatic estimates of 6 to 9 m a.s.l. for MIS 5e (Hearty et al., 2007; Dutton & Lambeck, 2012) could suggest tectonic overprinting. Some samples from these terraces also give older ages consistent with MIS 7 (200–240 ka), showing that Kish Island may host a polycyclic reef record in which different interglacial reef surfaces have been preserved at similar elevations. The estimated long-term uplift rates of 0.13 - 0.24 mm/yr for the island are determined on the combined MIS 5 and MIS 7 ages (Pirazzoli et al., 2004; Preusser et al., 2003).

3.1.2.2. Qeshm Island

Qeshm Island, the largest island in the Persian Gulf and located within the Strait of Hormuz (Fig. 2), preserves some of the most extensive and well-exposed late Quaternary marine terraces in the region, comprising up to 18 distinct terrace orders, with the highest reaching an elevation of 220 m a.s.l. All these terraces are mapped and dated (Reyss et al., 1998; Pirazzoli et al., 2004). The most reliable RSL indicators of the Last Interglacial highstand (MIS 5) from Qeshm Island are reef terraces and are situated between 10 and 26 m a.s.l. (from RSL_4517 to RSL_4526). These deposits consist of reefal limestones dominated by *Porites* and *Favia*, interbedded with lumachelle-rich limestones, barnacle-bearing beachrocks, and cemented bioclastic sands. The coral assemblages are typically preserved in situ. Such lithofacies are consistent with shallow subtidal to intertidal reef accretion and abrasion platforms.

Chronological control is obtained from a combination of U-series and ESR dating across the Qeshm Island. U-series ages from the terraces at 12–21 m a.s.l., yielded results of 139 ± 6 ka and 127 ± 6 ka, consistent with MIS 5e deposition. One terrace on Qeshm Island at 26.5 m a.s.l. yielded a U-series age of 104 ± 4 ka from corals in growth position, placing it in the MIS5c age and positioning that terrace above the MIS5e record observed by other studied sites on the island. This may be due to local tectonic activities (RSL_4522; Pirazzoli et al., 2004; Reyss et al., 1998). The overall ages at different elevations are further complemented with ESR dating (Pirazzoli et al., 2004), which confirmed age ranges 110–133 ka for corals at 10–21 m a.s.l., thereby reinforcing attribution of these reef terraces to MIS 5e. RSL

https://doi.org/10.5194/essd-2026-153
Preprint. Discussion started: 22 June 2026

indicators, such as corals in Qeshm, which are above 21 m a.s.l., were dated using ESR, and yielded 115-138 ka with an average age uncertainty of 12 ka, indicating that they may also correspond to MIS 5.

In addition, ESR results highlighted diagenetic complexities in some samples, but the overlap between U-series and ESR datasets provides robust chronological evidence for Last Interglacial reef growth on Qeshm. The elevation of these terraces is significantly higher than global eustatic benchmarks for MIS 5e (6 to 9 m a.s.l.; Hearty et al., 2007; Dutton & Lambeck, 2012), which led Reyss et al. (1998) to estimate an average uplift rates of 0.2 mm/yr since MIS 5 for that area. Thus, Qeshm Island provides a well-documented chronological control along a stratigraphically coherent record of the Last Interglacial in the Persian Gulf. Terraces at approximately 10–20 m a.s.l., constrained by overlapping U-series and ESR ages of 110–139 ka, record reef accretion during MIS 5e.

3.2 Oman

3.2.1 Northern Oman T3

The northeastern coast of Oman, between Quriyat and Qalhat (Fig. 2), exposes laterally extensive and morphologically well-preserved marine terraces. The late Quaternary deposits were first systematically documented by Hoffmann et al. (1999, 2007, 2013a,b, 2020), who recognized a preserved sequence of at least twelve terraces, of which the MIS 5 terraces (T1–T3) are the most prominent and well dated. The T3 terrace, archived in WALIS as RSL_4501, is correlated with the Last Interglacial (MIS 5e, 125 ka) and occurs consistently at elevations of 36 m a.s.l. Chronological control is provided by cosmogenic nuclide and optically stimulated luminescence (OSL) dating of associated sediments, both of which firmly place these deposits within MIS 5 in a broader context. In more precise terms, the two OSL ages (DEL4-Q and DEL5-Q) of 118 and 97 ka, respectively, fall within the limits of MI5e and MIS5c, while the cosmogenic nuclide dates of T3 are much older than MIS 5.

The lithological composition of T3 contains eight identified lithofacies and is grouped into six facies associations, ranging from foreshore cross-bedded sandstones and upper shoreface coarse conglomerates to mollusk-rich cemented beachrocks and carbonate-cemented gravels (Falkenroth et al., 2019). These deposits are formed in high-energy, foreshore to shallow shoreface, settings. The clear stratigraphic and sedimentological evidence, associated with age constraints, makes these deposits reliable sea-level index points for MIS 5e.

Two younger terraces, T2 (2 to 4 m a.s.l.) and T1 (1 to 2 m a.s.l.), might represent MIS 5c (100 ka) and MIS 5a (80 ka) highstands, respectively. Their presence alongside T3 provides evidence of Last Interglacial sea-level oscillations. The MIS 5 terraces in Oman provide one of the clearest records of Last Interglacial sea-level change within a tectonically uplifted setting. The lithofacies confirm deposition in shallow coastal environments, providing precise sea-level index points.

3.2.2 Sur lagoon

https://doi.org/10.5194/essd-2026-153
Preprint. Discussion started: 22 June 2026

Sur Lagoon is located on the northeastern coast of Oman, just below the Qalhat area (Fig. 2), and presents a laterally continuous bioerosional notch associated with the Last Interglacial. The notch, developed in fanglomerate bedrock, encircles the lagoon at a consistent elevation. It hosts an assemblage of biological markers, including mussel borings (*Gastrochaenolites* sp.), sponge borings (*Entobia* sp.), barnacle colonies, and oysters, that provide constraints on paleo sea level (Falkenroth et al., 2020). Differential GPS surveys place the notch apex at 3.93 ± 0.12 m a.s.l., indicating a MIS 5 highstand of about 4 m a.s.l. The attribution to MIS 5 is supported by cosmogenic nuclide ^{10}Be exposure dating of the underlying fanglomerate and is not reliable due to unknown precise values (Falkenroth et al., 2020). This notch is archived in WALIS as RSL_4541, with its indicative meaning tied to the intertidal zone and only minimal vertical uncertainty due to clear biological zonation.

A second indicator in the area consists of cemented beach deposits (beachrock). These deposits composed of intertidal sands cemented during early diagenesis, preserve bedding features that fix their indicative range to the intertidal zone. Optically stimulated luminescence (OSL) dating by Mauz et al. (2015) yielded an age of 80 ± 3 ka, correlating the beachrock with the MIS 5a highstand. This record is archived in WALIS as RSL_4502. Sur Lagoon offers one of the clearest Last Interglacial sea-level records in the Arabian Sea region, with reliable chronological control provided by Mauz et al. (2015) and methodological refinement by Falkenroth et al. (2020).

3.3 India

3.3.1 The Saurashtra Coast of Kathiwar Peninsula

The Saurashtra coast of western India (Fig. 1; Fig. 3) preserves Late Quaternary shorelines, with the coastal *miliolite* belt representing the most important evidence of marine transgression. These carbonate-rich deposits, locally known as *Porbandar Stone*, have been investigated by Brückner (1989) and later reassessed by Bhatt and Bhonde (2006).
At Porbandar and Tunkra (Fig. 1; Fig. 3), fossiliferous deposits crop out at 4 m a.s.l. (RSL_4540). The lithofacies is characterized by fossiliferous miliolite, a shallow-marine limestone containing mollusks assemblages (*Tellina*, *Cerithium*, *Ostrea*, *Area*), some of which are preserved in situ position. The skeletal assemblages include benthic foraminifera, ostracods, and bryozoans which confirms the deposition in intertidal to shallow-subtidal environments. These deposits occur at the base of the coastal miliolite succession and are overlain by aeolian dune carbonates, marking the regression that followed the Last Interglacial highstand (Brückner, 1989).
Chronological control is provided by U-series and ESR dating of shells of *Tellina,* which yielded ESR ages of 94.9 ± 10, 97.6 ± 10, and 105.0 ± 10 ka, consistent with attribution to MIS 5 (Brückner, 1989). U-series dating attempts were less reliable due to diagenetic alteration of *Tellina* shells. The inland miliolite formations, sometimes rising above 30–60 m a.s.l are dominantly aeolian in origin and not directly linked to sea level (Bhatt & Bhonde, 2006). The coastal miliolite belt preserves two distinct marine phases. The younger, marine-influenced generation (Miliolite-I) corresponds to the Last Interglacial transgression, while older miliolite formations (Miliolite-II and beyond) likely predate MIS 5 (Brückner, 1989).

https://doi.org/10.5194/essd-2026-153
Preprint. Discussion started: 22 June 2026

The coastal miliolite deposits of Saurashtra indicate that during the Last Interglacial highstand, sea level reached 4 m a.s.l. Thus, Saurasthra provides the western Indian reference site for the Last Interglacial sea level record consisting of faunal assemblages, marine lithofacies, and chronology.

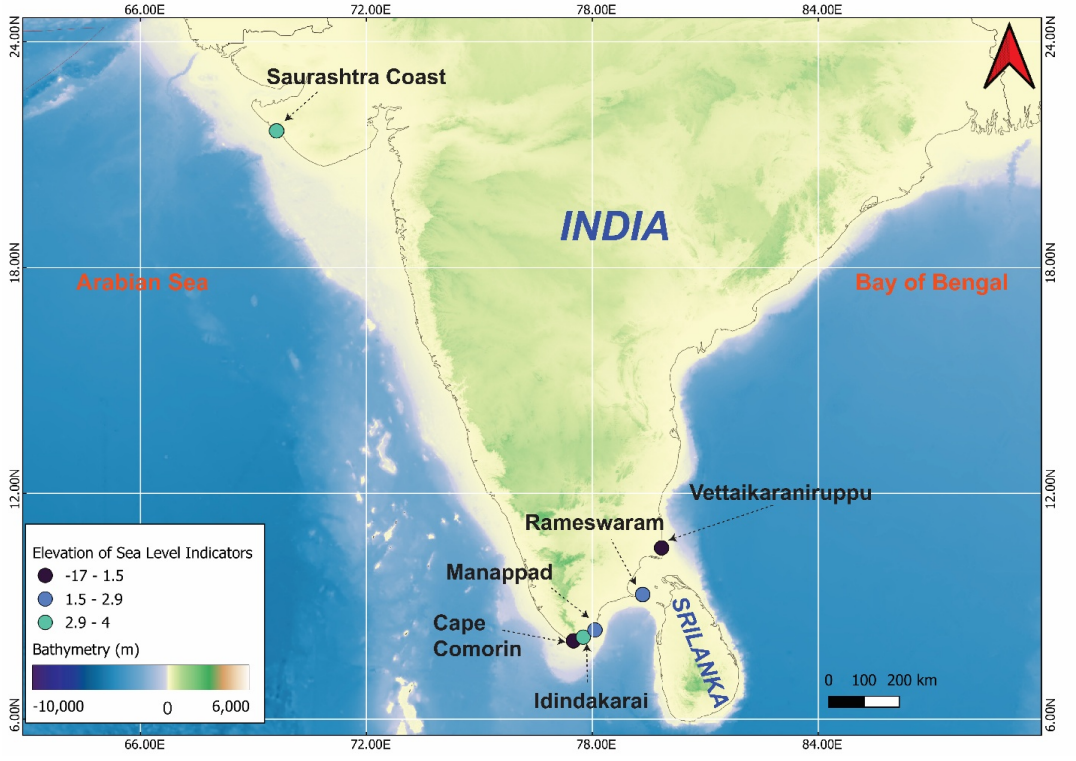

Figure 3 Map of the Indian Peninsula Last interglacial SLIPs. Colored dots represent sea-level data points included in the WALIS database, with colors indicating elevation. Basemap assembled from datasets provided by the Global Multi-Resolution Topography (GMRT).

3.3.2 Cape Comorin

At the southern extremity of the Indian peninsula, Cape Comorin (Fig. 3) has been investigated in detail by Brückner (1989), followed by Banerjee (2000). A site is located 6 km west of Cape Comorin, and the preserved Last Interglacial shoreline deposit consists of a cemented beach conglomerate (RSL_4492) that outcrops at an elevation of 1.2 m above low-tide level (LTL). The lithofacies is characterized by coarse beachrock facies, composed of clast-supported conglomerates cemented by sparry calcite. The deposit contains abundant shallow-water bioclasts, including marine shell fragments and foraminiferal tests. The skeletal assemblage is dominated by intertidal foraminifera (*Ammonia*, *Elphidium*, *Cibicides, Globigerinoides, Amphistegina, and Epinoides),* which shows the deposition in a high-energy

https://doi.org/10.5194/essd-2026-153
Preprint. Discussion started: 22 June 2026

foreshore environment. The presence of iron-oxide coatings on many bioclasts suggests brief episodes of subaerial exposure during or after deposition (Banerjee, 2000).

Dating of this unit was performed by using U-series analysis of marine shells. One specimen yielded a Th–U age of 112 ka +16/-14 (Brückner, 1989; Banerjee, 2000). Although mollusks are generally less reliable due to uranium exclusion and susceptibility to diagenesis, the age is stratigraphically matched with the regional Last Interglacial patterns. Radiocarbon attempts on the same facies produced anomalously young ages, attributed to secondary carbonate overprinting (Banerjee, 2000). The Cape Comorin beachrock (RSL_4492) provides a Last Interglacial index point combining lithofacies evidence of intertidal deposition with a U-series chronology of 112 +16/-14 ka.

3.3.3 Idindakarai

This site is located 35 km northeast of Cape Comorin on the Gulf of Mannar margin and preserves one of the most prominent Last Interglacial shoreline successions described along the Tamil Nadu coast (Fig. 1; Fig. 3). The site was first documented by Brückner (1989), who identified a marine terrace elevated between 3 and 5 m above LTL. The re-investigations by Banerjee (2000) provided a more detailed stratigraphy and depositional environment, confirming its correlation with the Last Interglacial highstand (MIS 5e) (RSL_4493).

The lower, 1.5 m thick, cross-laminated grainstone sequence is characterized by ripple bedding sealed with bioturbated contact, which is interpreted as foreshore to shoreface in origin. This is overlain by a 0.6 - 1.0 m thick grainstone facies containing abundant mollusk bioclasts, peloids, and borings produced by intertidal organisms such as *Balanus*. This facies indicates a deposition in a shallow, high-energy intertidal environment

Chronological control is determined from U-series analysis of marine shells. Brückner (1989) reported an age of approximately 124 +14/-8 ka, and Banerjee (2000) confirmed the assignment of this terrace to MIS 5e. However, mollusks are problematic substrates for U-series dating, as they generally incorporate little uranium during life and are prone to diagenetic alteration (Kaufman et al., 1971). Despite these uncertainties, the stratigraphic position, elevation (3.4 m a.s.l.; RSL_4493), and faunal evidence strongly support attribution to the Last Interglacial.

3.3.4 Manappad

The Manappad site is located about 40 km northeast of Idindakarai on the southeast Indian coast (Fig. 1; Fig. 3) and preserves a well-defined sequence of marine terraces formed during the Late Pleistocene. Brückner (1989) described a series of stepped marine terraces in this area, with the major focus on the marine terrace level (T2) at 2-3 m above LTL. Later, Banerjee (2000) re-examined the same succession and suggested that the T2 terrace belongs to the Last Interglacial based on U-series dating

The T2 terrace is formed by consolidated beach deposits and beachrock facies. The lithofacies consist of well-cemented, grain-supported conglomerates containing marine shell fragments and barnacle encrustations. A key indicator an in situ *Balanus* sp., confirming the intertidal origin of the deposit (Banerjee, 2000). The elevation of marine terrace T2 is reported at 2.15 m above LTL (RSL_4494).

https://doi.org/10.5194/essd-2026-153
Preprint. Discussion started: 22 June 2026

Chronological control was attempted by using U-series dating on the marine shell *Balanus* sp. Although the analytical results were not always internally consistent due to diagenetic alteration of the shells, Banerjee (2000) correlated this terrace with MIS 5e based on its stratigraphic position, elevation, and comparison with nearby dated sites at Idindakarai and Cape Comorin. Brückner (1989) had already suggested the same correlation. The Manappad terrace, therefore, provides additional evidence for a Last Interglacial highstand at 2 m above LTL along the Tamil Nadu passive margin.

3.3.4 Rameshwaram

The island of Rameswaram, located in the Gulf of Mannar (Tamil Nadu, India, Fig. 1; Fig. 3), provides a rare archive of Last Interglacial sea-level indicators along the passive southeastern continental margin of the Indian Peninsula. Situated at the northern end of Adam's Bridge, Rameswaram is geomorphologically characterized by low-lying marine terraces, fossil coral colonies, and associated carbonate facies. This locality was first examined by Brückner (1989) using chronological methods that include U-series dating and ESR. Later, this locality was further investigated by Banerjee (2000), who presented additional U-series chronology, confirming the presence of multiple Last Interglacial reefal sea level indicators at a maximum elevation of 2.9 m above LTL. Later, Loveson and Nigam (2019) discussed Rameswaram's Last Interglacial coral-bearing sea level proxies and their chronological constraints in their review. These sites are now archived in WALIS (RSL_4489, RSL_4490, RSL_4491, RSL_4503, RSL_4504, RSL_4505, and RSL_4506).

On the northern coast at Narikulam (Rameswaram), an *Acropora* colony of 1 m^2 sq in situ (RSL_4489) is present at an elevation of 1.1 m above LTL. This coral yielded a Th–U (alpha count) age of 125.6 ± 8.5/7.5 ka, closely corresponding to global MIS 5e. However, minor detrital contamination and diagenetic alteration may affect the precision of the dating (Banerjee, 2000). The 100m patch of *Acropora* colony is present, which gradually disappears, while a large *Porites* colony becomes dominated and associated with *Diploastrea*, *Cycloseris,* and *Goniopora* (RSL_4490, RSL_4491, RSL_4503, RSL_4504, RSL_4505, and RSL_4506). The elevation of this coral terrace (T2) ranges between 2.4 and 2.9 m above LTL. Several *Porites* samples reflect U/Th (Alpha count) ages ranging from 92 to 116 ka. While some specimens show a recrystallization into coarse-fibrous aragonite and localized calcite replacement, the stratigraphic coherence and clustering of ages strongly support their correlation with MIS 5.

The coral terraces dominated by *Porites* extend laterally for several kilometers, covering 10 km^2 in the case of the Pisasu Munai complex, and form a prominent flat surface dissected by seasonal monsoonal flooding. The repeated monsoon flooding accelerated diagenetic alteration in these corals, explaining the prevalence of secondary mineralization (Brückner, 1989; Plaziat et al, 2008). However, the presence of primary aragonite fractions in several samples confirms that the ages are reliable (Gischler et al., 2008a; 2018a,b; Henderson et al., 1993).

The Rameswaram documents a Last Interglacial highstand between 2 to 3 m a.s.l., constrained by multiple in situ coral colonies dated between 92 and 125 ka (RSL_4489, RSL_4490, RSL_4491, RSL_4503, RSL_4504, RSL_4505, and RSL_4506), and stands as a reference locality for passive margin sea-level studies of the Last Interglacial.

https://doi.org/10.5194/essd-2026-153
Preprint. Discussion started: 22 June 2026

3.3.5 Vettaikaraniruppu

The Vettaikaraniruppu site is situated on the southeast coast of India (Tamil Nadu, India). The Last Interglacial sea level record was first reported by Goswami et al. (2019), who investigated the beach ridge through a drill core (VKI core). The core provided detailed subsurface stratigraphy of the Last Interglacial (MIS 5e) marine transgression from the Kaveri delta. The coring site is located at 7 m a.s.l *(*RSL_4539).

The VKI core revealed a complete succession of silty sands, organic-rich clays, and carbonate-rich grainstones. The basal sandy layers displayed cross-laminated and ripple bedding, typical of foreshore to shoreface facies deposited under high-energy wave and swash processes. At a depth of 21-21.5 m b.s.l., the organic-rich sandy clays were recovered, representing low-energy conditions, likely associated with lagoonal or back-barrier settings that developed during the landward shift of environments in the marine transgression.

The upper part of the core consists of carbonate-rich grainstones with abundant marine shell debris and benthic foraminifera that includes shallow-marine skeletal assemblages. These faunal assemblages confirm the deposition in an intertidal to shallow subtidal setting during the peak of the highstand.

Chronological constraints are determined for the VKI core sandy clay layer at 21-21.5 m b.s.l., using Optically stimulated luminescence (OSL) dating, and yielded an age of 121 ± 11 ka, which correlates the sequence with the Last Interglacial highstand (MIS 5e). The stratigraphy of the core demonstrates a marine transgression during MIS5e, beginning with foreshore sands, passing through lagoonal clays, and culminating in shallow-marine carbonate grainstones.

Thus, the VKI core at Vettaikaraniruppu provides one of the clearest stratigraphic archives of the MIS 5e transgression along the southeast Indian margin, combining geomorphological evidence of beach ridges with subsurface lithofacies and an OSL chronology.

3.4 Indian Ocean

3.4.1 Maldives archipelago

Rasdhoo Atoll, situated in the central Maldives archipelago (Fig. 1), represents one of the very few documented sites in the equatorial Indian Ocean where Last Interglacial (MIS 5e) reefal deposits have been identified and dated. The succession, described by Gischler et al. (2008a) and revisited in later works (Gischler et al., 2008b; 2018a), is preserved at 14.5 m b.s.l. and is archived in the WALIS database as RSL_4495, RSL_4498, RSL_4537, and RSL_4538. The deposits consist of coralgal grainstones dominated by *Isopora palifera* and *Acropora gr. robusta*, with additional contributions from encrusting *Porites*, *Leptoseris*, coralline algae (*Porolithon onkodes*), and vermetids, indicating formation in a shallow back-reef environment with paleo-water depths of less than 10 m.

Chronological control is provided by U-series dating of acroporid corals. A well-preserved specimen yielded a reliable age of 136.9 ± 2.0 ka, while two further ages of 114.3 ± 1.5 ka and 117.3 ± 2.7 ka are considered moderately reliable

https://doi.org/10.5194/essd-2026-153
Preprint. Discussion started: 22 June 2026

due to partial diagenetic alteration (Gischler et al., 2008a, b). Later work reported two additional ages close to 151 ka, but these are regarded as unreliable owing to anomalous $^{234}U/^{238}U$ signatures (Gischler et al., 2018a). Despite these limitations, the stratigraphic and clustering of ages firmly link the Rasdhoo deposits to MIS 5e. The coralgal deposits which are dated with U-series ages and yielded between 114 and 137 ka, are positioned at 14.5 m b.s.l., demonstrate that even globally synchronous highstands can be significantly modified by local tectonics. As archived in WALIS (RSL_4495, RSL_4498, RSL_4537, RSL_4538), these data provide an essential reference point for reconstructing subsidence-corrected relative sea-level histories in low-lying carbonate platforms.

3.4.2 Cocos (Keeling) Islands

The Cocos (Keeling) Islands, located on the Cocos Rise in the eastern Indian Ocean (Fig. 1), provide one of the few well-dated archives of Last Interglacial (MIS 5e) reef deposits from an isolated oceanic atoll setting. This locality is geomorphologically characterized by lithified reef limestones overlain by unconsolidated Holocene sands and coralline limestones beneath the modern reef islands. The site was described by Woodroffe et al. (1991) based on borehole drilling and later explained within a broader Indian Ocean context by Woodroffe (2005). These deposits are archived in WALIS under RSL_4496.

Drilling across the atoll rim revealed a sharp discontinuity at 8–11 m b.s.l., separating poorly consolidated Holocene sediments from a well-lithified reef limestone. Within this older reef, a massive *Faviid* coral from 10.5 m b.s.l. yielded U-series ages of 118 ± 7 ka (bulk sample) and 123 ± 7 ka (secondary cement removed), confirming the formation during the Last Interglacial highstand (Woodroffe et al., 1991). The deposits consist mainly of coralline limestones with abundant massive *Faviid* corals and other reefal taxa, consistent with a shallow-water reef crest environment.

The Cocos (Keeling) Islands record documents a Last Interglacial reefal unit now situated 8–11 m b.s.l., constrained by U-series ages of 118–123 ka. The deposits, represented in WALIS as RSL_4496, provide key evidence of both MIS 5e reef development and sustained atoll subsidence in the eastern Indian Ocean, underscoring the importance of integrating tectonic corrections into regional sea-level reconstructions.

4. Discussion

The SLIPs in our database indicate that, along the coasts of Iran, Oman, India, Maldives, and Cocos Keeling Islands, there are significant departures from eustasy, caused by differential vertical land motions (Fig. 4) as this area includes an active convergent margin, a passive continental margin and an intraplate oceanic setting. When arranged longitudinally, the RSL index points in our database an elevation gradient transitioning from the uplifted active margins of Iran and Oman (where SLIPs indicate RSL up to 60 m a.s.l.), to a stable passive margin in India, with SLIPs indicating RSL at 1–4 m a.s.l. The subsidence pattern of the oceanic reef platforms of Maldives and Cocos islands is reflected in the RSL recorded at these sites, reaching maximum depths of 17 m b.s.l.

https://doi.org/10.5194/essd-2026-153
Preprint. Discussion started: 22 June 2026

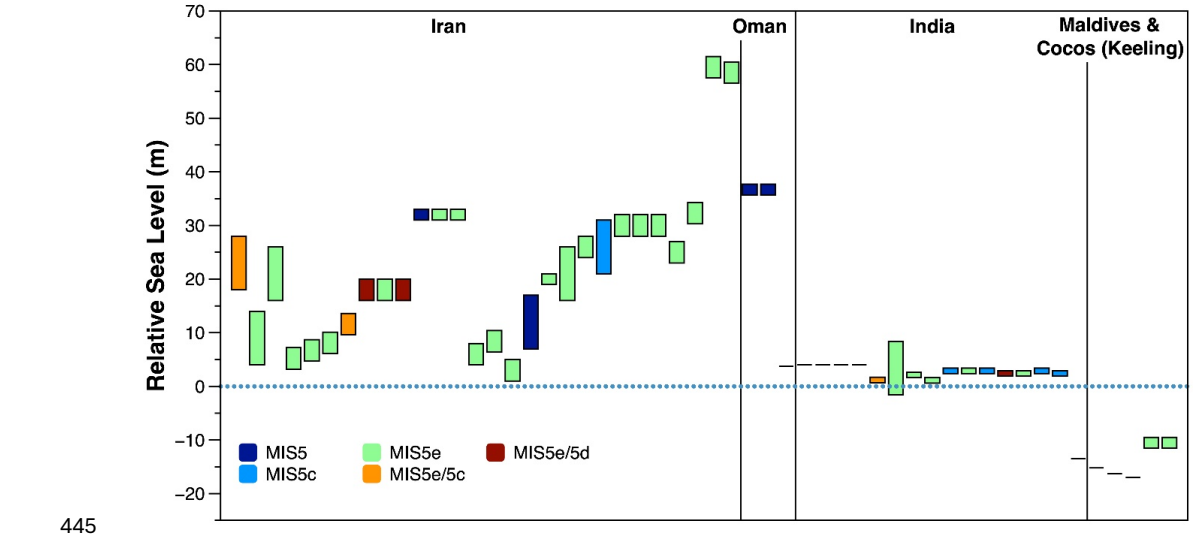

Figure 4 MIS 5 RSL elevation as indicated by SLIPs in our database across four major regions of the northern Indian Ocean: southern Iran, northern Oman, peninsular India, the Maldives, and Cocos (Keeling) Islands.

4.1.1 Uplifted Active Margins of Iran and Oman

Southern Iran displays notably high MIS 5 marine terraces. The elevated MIS 5c sea level indicators, mainly coral terraces reaching up to 23 m a.s.l. at the Haleh and Jazeh area, strongly suggest the influence of regional tectonic uplift, which is coherent with regional tectonic along the Zagros foreland fold-and-thrust-belt, where a long-term uplift rate of 0.2 mm/yr has been calculated (Reyss et al., 1998). This is consistent with values derived from other localities in southern Iran (Reyss et al., 1998; Pirazzoli et al., 2004; Preusser et al., 2003; Talebian & Jackson, 2002; Regard et al., 2004). The relative sea-level positions in this part of the Persian Gulf cannot be explained by eustasy alone and must be understood within a framework of steady Quaternary uplift combined with local salt diapirism processes.

Similarly, the MIS 5 sea level record of the Kish and Qeshm islands of southern Iran is also elevated up to 32 m a.s.l. These high elevations are explained by a steady uplift rate in the region, which has been attributed to salt doming and neotectonic activity in the southern Zagros foreland with an uplift rate of 0.6 mm/yr (Pirazzoli et al.,2004). This also explains why corals of different ages are found at elevations well above global eustatic benchmarks. The lower reef terraces of Kish Island at 5–12 m a.s.l. provide the clearest evidence of the Last Interglacial sea-level highstand, with coral facies and consistent ESR. The higher terraces containing MIS 5 corals are interpreted as Quaternary uplifted deposits whose present elevations reflect both reef accretion during MIS 5e and subsequent tectonic displacement. In this way, the Kish and Qeshm Islands provide stratigraphically coherent archives of MIS 5e sea level in the Persian Gulf, while also highlighting the importance of tectonic processes in shaping Quaternary coastal geomorphology in the region (Preusser et al., 2003; Pirazzoli et al., 2004; Hearty et al., 2007; Dutton & Lambeck, 2012).

https://doi.org/10.5194/essd-2026-153
Preprint. Discussion started: 22 June 2026

Moving eastward to the Makran coast (Konarak, Ramin, Lipar), MIS 5e terraces reach up to 60 m a.s.l., consistent with uplift rates of 0.15–0.25 mm/yr (Normand et al., 2019; Regard et al., 2004). These values reflect forearc deformation linked to the Makran Subduction Zone, where the Indian Plate is subducting beneath Eurasia (Byrne et al., 1992; Ellouz-Zimmermann et al., 2007). The preservation of MIS 5c and 5a terraces at lower elevations indicates punctuated uplift episodes superimposed on a steady long-term crustal rise.

In northern Oman, MIS5e sea level indicators occur up to 37 m a.s.l. following a similar uplift pattern of Kish and Qeshm island, with an uplift rate up to 0.2 mm/yr (Hoffmann et al., 2013, 2020; Decker et al.,2024). Local change near the Qualhat Fault, where terraces tilt up to 55 m over short distances, demonstrates active late Quaternary deformation associated with the Makran forebulge (Foubert et al., 2018). Despite this uplift, the Sur Lagoon notch (3.9 m a.s.l.; RSL_4541) and 80 ± 3 ka beachrock (RSL_4502) correspond closely to the global MIS 5e and 5a highstands, respectively, confirming near-eustatic conditions locally. These records form an uplifted but stratigraphically consistent archive of Late Quaternary sea-level change, underscoring the requirement for uplift correction when comparing to global curves (Dutton et al., 2015a; Rovere et al., 2016a).

4.1.2 Peninsular India: A Tectonically Stable to Slightly Subsiding Passive Margin

The Indian coastal region displays a completely different tectonic setting compared to southern Iran and the northern Oman region (Fig. 2). Along the Saurashtra coast of western India and the southeastern Tamil Nadu coast, which includes Cape Comorin Idindakarai, Manapad, and Rameswaram, MIS 5e indicators lie at 1–4 m a.s.l. (Brückner, 1989; Banerjee, 2000; Rajendran et al., 2013). These elevations, in line with GMSL estimates, suggest a tectonically stable passive margin, possibly subjected only to minor uplift/subsidence due to tectonics of glacial isostatic adjustment response to loading and unloading of the Indian Ocean basin (Banerjee, 2000; Milne et al., 2009). Hydro-isostatic models predict that continental shelves near large oceanic basins subside by several meters in response to the relaxation of peripheral forebulges following deglaciation (Farrell & Clark, 1976; Lambeck et al., 2014). The uniform low-elevation MIS 5e indicators across southern India fit this model, implying minimal tectonic perturbation during the Last Interglacial. Stratigraphic and sedimentological evidence, like beach ridges, marine terraces and shallow-marine fauna, support a marine transgression during MIS5e in the southern Indian region (Banerjee, 2000). Thus, peninsular India provides a regional baseline against which uplifted or subsiding settings in the Indian Ocean can be calibrated.

4.1.3 Subsiding Oceanic Platforms: Maldives and Cocos (Keeling)

The Maldives Archipelago and Cocos (Keeling) Islands define the subsiding endmember of the Indian Ocean system. Last Interglacial coral frameworks from the Maldives occur up to 17 m b.s.l., suggesting subsidence rates of 0.09–0.16 mm/yr (Gischler et al., 2018a). These rates exceed simple thermal contraction values for 60–80 Ma oceanic lithosphere (Parsons & Sclater, 1977), suggesting additional tectonic or flexural loading components (Woodroffe,

https://doi.org/10.5194/essd-2026-153
Preprint. Discussion started: 22 June 2026

2005). Submergence of MIS 5e reefs also reflects limited accommodation space and continuous platform down-warping (Purdy & Bertram, 1993; Perry et al., 2008). At Cocos (Keeling), submerged coral heads at 10 m b.s.l. yield ages of 123 ka, consistent with subsidence rates of 0.1–0.12 mm/yr (Woodroffe et al., 1991; Woodroffe, 2005). These rates, higher than expected for pure lithospheric cooling, may record lithospheric flexure associated with the Wharton Ridge or long-term dynamic topography of the Indian Ocean basin (Müller et al., 2008; Hoggard et al., 2016). Hence, both the Maldives and Cocos records confirm that the apparent depth of MIS 5e reefs is dominated by subsidence.

5. Conclusions

This review presents the first standardized Last Interglacial (MIS 5) relative sea-level record spanning the South Asian and Indian Ocean regions, extending from Iran, Oman, India, to the Maldives, and the Cocos (Keeling) Islands. By integrating 54 sea level indicators from 17 peer-reviewed studies into the WALIS framework, we reassessed stratigraphic context, depositional environments, elevation accuracy, and chronological control using U-series, ESR, luminescence, and cosmogenic dating. The resulting dataset reveals strong regional contrasts driven primarily by different tectonic settings. Active margins in southern Iran and northern Oman preserve MIS 5e, 5c, and 5a marine terraces, with elevations up to 60 m a.s.l., reflecting uplift associated with the Zagros fold-and-thrust belt, salt tectonics, and the Makran subduction system. On the other hand, the passive margin of western and southern India shows MIS 5e sea level indicators at 1–4 m a.s.l., consistent with tectonic stability. However, the MIS 5e reefs in the Maldives and Cocos (Keeling) Islands lie 10–17 m below present sea level, showing a late Quaternary subsidence of oceanic platforms. Furthermore, the identification of MIS 5c and MIS 5a highstands in uplifted settings, such as Oman and the Makran coast, demonstrates that South Asia and the northern Indian Ocean preserve key evidence of the youngest MIS 5 sea-level oscillations.

Overall, this study provides standardized information for reconstructing Last Interglacial sea level changes in a region that has been historically underrepresented in global databases.However, significant data gaps remain along the Pakistan margin, where the lack of detailed and consistently documented studies currently prevents the inclusion of reliable, standardized sea-level datapoints, highlighting the need for targeted future investigations. The standardized dataset provides an essential reference for future modeling of glacio-hydro-isostatic processes, vertical land motion, and Indian Ocean tectonics studies. Importantly, the reviewed sea level records offer valuable analogues for understanding how coastlines with varied tectonic and geomorphic settings may respond to future sea-level rise.

6. Data availability

The South Asia and the Indian Ocean database is available at https://doi.org/10.5281/zenodo.18512770 (Version 1; Ali et al.,2026). The description of the database fields can be found at https://zenodo.org/record/ 3961544 (Rovere et al., 2020)

https://doi.org/10.5194/essd-2026-153
Preprint. Discussion started: 22 June 2026

Open Access Earth System Science Data Discussions

Acknowledgements

This study is an outcome of the WARMCOAST project, funded by the European Research Council (ERC) under the European Union's Horizon 2020 research and innovation programme (Grant agreement No. 802414). The authors are particularly grateful to the Department of Environmental Sciences, Informatics and Statistics (Ca' Foscari University of Venice) for technical support during the project. The authors are also thankful to the WALIS database contributors.

Funding

This paper is a result of the WARMCOAST project, funded by the European Research Council (ERC) under the European Union's Horizon 2020 research and innovation programme (Grant agreement No. 802414). This paper reflects only the author's view and that the EU is not responsible for any use that may be made of the information it contains.

Author contributions

Mubashir Ali & Ciro Cerrone; Investigation, Conceptualization, writing the original draft, visualization.
Alessio Rovere: Conceptualization, writing the original draft, Supervision, and visualization.

Competing interests

The authors declare that they have no known competing financial interests or personal relationships that could have appeared to influence the work reported in this paper. At least one of the (co-)authors is a member of the editorial board of Earth System Science Data.

References

Ali, M., Cerrone, C., Rovere, A., 2026. A review of last interglacial sea-level proxies in South Asia and the Indian Ocean, Zenodo [data set], https://doi.org/10.5281/zenodo.18512770, 2026

Antonioli, F., Lo Presti, V., Rovere, A., Ferranti, L., Anzidei, M., Furlani, S., Mastronuzzi, G., Orru, P. E., Scicchitano, G., Sannino, G., Spampinato, C. R., Pagliarulo, R., Deiana, G., de Sabata, E., Sansò, P., Vacchi, M., and Vecchio, A.: Tidal notches in Mediterranean Sea: a comprehensive analysis, Quaternary Science Review, 119, 66–84, https://doi.org/10.1016/j.quascirev.2015.03.016, 2015.

Banerjee, P.: Late Quaternary sea-level highstands along the east coast of India. Journal of the Geological Society of India, 55(2), 181–194, 2000

https://doi.org/10.5194/essd-2026-153
Preprint. Discussion started: 22 June 2026

Bhatt, N., & Bhonde, U.: Geomorphic expression of late Quaternary sea level changes along the southern Saurashtra coast, western India. *Journal of earth system science*, *115*(4), 395-402, 2006

Bird, P.: An updated digital model of plate boundaries. G-cubed 4 (3)., 2003

Boyden, P., Weil-Accardo, J., Deschamps, P., Oppo, D., and Rovere, A.: Last interglacial sea-level proxies in East Africa and the Western Indian Ocean, Earth Syst Sci Data, 13, 1633–1651, 2021

Brückner, H.: Late Quaternary shorelines and sea-level changes along the coasts of India. Zeitschrift für Geomorphologie, 33(1), 3–16, 1989.

Byrne, D. E., Davis, D. M., & Sykes, L. R.: Loci and maximum size of thrust earthquakes and the mechanics of the shallow region of subduction zones. Journal of Geophysical Research, 97(B4), 449–478, 1992

Decker, N., Hoffmann, G., Al-Kindi, A., & Frechen, M.: Uplifted Late Quaternary marine terraces along the Omani coast: Implications for the forebulge of the Makran subduction zone. Quaternary Science Reviews, 326, 108035, 2024

Dutton, A., & Lambeck, K.: Ice volume and sea level during the Last Interglacial. Science, 337, 216–219, 2012

Dutton, A., Webster, J.M., Zwartz, D., Lambeck, K., & Wohlfarth, B.: Sea-level variability in the last interglacial: A global perspective. Earth and Planetary Science Letters, 409, 143–153. https://doi.org/10.1016/j.epsl.2014.10.018, 2015a

Ellouz-Zimmermann, N., Deville, E., Müller, C., Leturmy, P., & Rudkiewicz, J.-L.: The tectonic structure and evolution of the Makran accretionary wedge. Tectonics, 26(5), TC5019, 2007

Falkenroth, M., Schneider, B., & Hoffmann, G.: Beachrock as sea-level indicator – A case study at the coastline of Oman (Indian Ocean). Quaternary Science Reviews, 206, 81–98. https://doi.org/10.1016/j.quascirev.2019.01.003, 2019

Falkenroth, M., Adolphs, S., Cahnbley, M., Bagci, H., Kázmér, M., Mechernich, S., & Hoffmann, G.: Biological indicators reveal small-scale sea-level variability during MIS 5e (Sur, Sultanate of Oman). *Open Quaternary*, *6*(1), 2020

Farrell, W. E., & Clark, J. A.: On postglacial sea level. Geophysical Journal of the Royal Astronomical Society, 46(3), 647–667, 1976

https://doi.org/10.5194/essd-2026-153
Preprint. Discussion started: 22 June 2026

Foubert, A., Hasiotis, T., & Hoffmann, G.: Quaternary marine terraces and their significance along the northern Oman coast. Sedimentology, 65(1), 175–197, 2018

Garzón, S. and Rovere, A.: WALIS dashboard: An online tool to explore a global paleo sea-level database, Open Research Europe, 3, 114, https://doi.org/10.12688/openreseurope.16183.2, 2024.

Gischler, E., Hudson, J.H., & Pisera, A.: Late Quaternary reef growth and sea level in the Maldives (Indian Ocean). Marine Geology, 250, 104–113. https://doi.org/10.1016/j.margeo.2008.01.004, 2008a

Gischler, E.: Corrigendum to "Late Quaternary reef growth and sea level in the Maldives (Indian Ocean)." Marine Geology, 255, 102. https://doi.org/10.1016/j.margeo.2008.07.002, 2008b

Gischler, E., Humblet, M., Braga, J.C., & Eisenhauer, A.: Last interglacial reef facies and late Quaternary subsidence in the Maldives, Indian Ocean. Marine Geology, 406, 34–41, 2018a

Gischler, E., Hudson, J. H., & Oschmann, W.: Late Quaternary sea-level and environmental changes in the Maldives (Indian Ocean): Evidence from reef structures and sediments. Quaternary Science Reviews, 200, 180–197, 2018b

Goswami, K., Krishnan, S., Kumerasan, A., Sadasivam, S.K., Kumar, P., & Jaiswal, M.K.: Luminescence chronology of fluvial and marine records from subsurface core in Kaveri delta, Tamil Nadu: Implications to sea level fluctuations. *Geochronometria*, *46*(1), 125-137, 2019

Hearty, P. J., Hollin, J. T., Neumann, A. C., O'Leary, M. J., & McCulloch, M.: Global sea-level fluctuations during the Last Interglaciation (MIS 5e). Quaternary Science Reviews, 26, 2090–2112, 2007

Henderson, G. M., Cohen, A. S., & O'nions, R. K.: $^{234}U/^{238}U$ ratios and230Th ages for Hateruma Atoll corals: implications for coral diagenesis and seawater234U/238U ratios. Earth and Planetary Science Letters, 115(1-4), 65-73, 1993

Hoffmann, G., Al-Saifi, M., Al-Battashi, M., & Grützner, C.: Raised marine terraces and Quaternary sea-level changes along the coast of Oman. Quaternary International, 55, 39–49, 1999

Hoffmann, G., Al-Saifi, M., & Al-Battashi, M.: Quaternary marine terraces of the northeastern Oman coast: archives of climate and sea-level changes. Zeitschrift für Geomorphologie, 51(4), 441–467, 2007

https://doi.org/10.5194/essd-2026-153
Preprint. Discussion started: 22 June 2026

Hoffmann, G., Reicherter, K., Wiatr, T., Grützner, C., & Rausch, T.: Block rotation and neotectonic extension at the passive continental margin of Oman, NW Indian Ocean. Tectonics, 32(4), 660–675. https://doi.org/10.1002/tect.20046, 2013a

Hoffmann, G., Al-Kindi, A., & Brückner, H.: Uplifted coral terraces and the tectonic evolution of the northeastern Oman coast. Quaternary Research, 79(3), 325–340, 2013b

Hoffmann, G., Wenzel, F., Reicherter, K., Grützner, C., & Wiatr, T.: Uplifted marine terraces and neotectonics along the northern Oman coast. Geomorphology, 351, 106957, 2020

Hoggard, M. J., White, N., & Al-Attar, D.: Global dynamic topography observations reveal limited influence of large-scale mantle flow. Earth and Planetary Science Letters, 449, 255–268, 2016

Kaufman, A., Broecker, W. S., Ku, T. L., & Thurber, D. L.: The status of U-series methods of mollusk dating. Geochimica et Cosmochimica Acta, 35(11), 1155-1183, 1971

Khan, N. S., Horton, B. P., Engelhart, S., Rovere, A., Vacchi, M., Ashe, E. L., Törnqvist, T. E., Dutton, A., Hijma, M. P., and Shennan, I.: Inception of a global atlas of sea levels since the Last Glacial Maximum, Quat Sci Rev, 220, 359–371, https://doi.org/10.1016/j.quascirev.2019.07.016, 2019.

Lambeck, K., Rouby, H., Purcell, A., Sun, Y., & Sambridge, M.: Sea level and global ice volumes from the Last Glacial Maximum to the Holocene. Proceedings of the National Academy of Sciences, 111(43), 15296– 15303, 2014
Lorscheid, T. and Rovere, A.: The indicative meaning calculator quantification of paleo sea-level relationships by using global wave and tide datasets, Open Geospatial Data Software and Standards, 4, https://doi.org/10.1186/s40965-019-0069-8, 2019.

Loveson, V. J., & Nigam, R. (2019). Reconstruction of Late Pleistocene and Holocene sea level curve for the east coast of India. Journal of the Geological Society of India, 93(5), 507-514.

Mauz, B., Vacchi, M., Green, A., Hoffmann, G., and Cooper, A.: Beachrock: a tool for reconstructing relative sea level in the far-field, Mar Geol, 362, 1–16, 2015a.

Mauz, B., Zander, A., Brückner, H., & Masrour, M.: Last Interglacial coastal environments in Oman: A robust sea-level indicator from notches and beachrocks. Marine Geology, 366, 71–82, 2015b.

Milne, G. A., Gehrels, W. R., Hughes, C. W., & Tamisiea, M. E.: Identifying the causes of sea-level change. Nature Geoscience, 2(7), 471–474, 2009

https://doi.org/10.5194/essd-2026-153
Preprint. Discussion started: 22 June 2026

Müller, R. D., Sdrolias, M., Gaina, C., & Roest, W. R.: Age, spreading rates and spreading asymmetry of the world's ocean crust. Science, 319(5863), 1357–1362, 2008

Normand, C., Nazari, H., Lahijani, H., Moussavi-Harami, R., Rastegar, A., Collina-Girard, J., Reyss, J.-L., & Gasse, F.: Quaternary sea-level markers along the Iranian Makran coast. Quaternary International, 528, 60–75, 2019.

Otvos, E. G.: Beach ridges—definitions and significance, Geomorphology, 32, 83–108, 2000.

Parsons, B., & Sclater, J. G.: An analysis of the variation of ocean floor bathymetry and heat flow with age. Journal of Geophysical Research, 82(5), 803–807, 1977.

Pedoja, K., Husson, L., Johnson, M. E., Melnick, D., Witt, C., Pochat, S., Nexer, M., Delcaillau, B., Pinegina, T., Poprawski, Y., Authemayou, C., Elliot, M., Regard, V., and Garestier, F.: Coastal staircase sequences reflecting sea-level oscillations and tectonic uplift during the Quaternary and Neogene, Earth Sci Rev, 132, 13–38, https://doi.org/https://doi.org/10.1016/j.earscirev.2014.01.007, 2014

Perry, C. T., Spencer, T., & Kench, P. S. (2008). Carbonate budgets and reef production states: a geomorphic perspective on the ecological phase-shift concept. Coral Reefs, 27(4), 853-866.

Pirazzoli, P. A., Reyss, J.-L., Fontugne, M., Haghipour, A., Hilgers, A., Kasper, H. U., Nazari, H., Preusser, F., & Radtke, U.: Quaternary coral-reef terraces from Kish and Qeshm Islands, Persian Gulf: new radiometric ages and tectonic implications. Quaternary International, 120, 15–27, 2004.

Pirazzoli, P. A.: Marine Terraces. Enclyclopedia of Coastal Science, Springer, 632–633, 2005.

Plaziat, J. C., Reyss, J. L., Choukri, A., & Cazala, C.: Diagenetic rejuvenation of raised coral reefs and precision of dating. The contribution of the Red Sea reefs to the question of reliability of the Uranium-series datings of middle to late Pleistocene key reef-terraces of the world. Carnets de Géologie/Notebooks on Geology, (A04), 1-35, 2008.

Preusser, F., Radtke, U., Fontugne, M., Haghipour, A., Hilgers, A., Kasper, H. U., Nazari, H., & Pirazzoli, P. A.: ESR dating of raised coral reefs from Kish Island, Persian Gulf. Quaternary Science Reviews, 22, 1317–1322, 2003

Purdy, E. G., & Bertram, G. T.: Carbonate concepts from the Maldives, Indian Ocean. AAPG Studies in Geology, 57, 1–56, 1993.

Rajendran, C. P., Rajendran, K., & Andrade, V.: Palaeotsunami evidence from the southern coast of India: Implications for historical records. Quaternary International, 298, 31–44, 2013

https://doi.org/10.5194/essd-2026-153
Preprint. Discussion started: 22 June 2026

Regard, V., Bellier, O., Thomas, J.-C., Bourlès, D., & Bonnet, S.: Cumulative right-lateral fault slip rate across the Zagros–Makran transfer zone. Geophysical Journal International, 158(1), 1–22, 2004

Reyss, J.-L., Pirazzoli, P. A., Haghipour, A., Hatté, C., & Fontugne, M.: Quaternary marine terraces and tectonic uplift rates on the south coast of Iran. In: Stewart, I.S. & Vita-Finzi, C. (eds) Coastal Tectonics. Geological Society, London, Special Publications, 146, 225–237, 1998

Rovere, A., Stocchi, P., & Vacchi, M.: Eustatic and relative sea level changes. Earth-Science Reviews, 155, 191–219, 2016a

Rovere, A., Raymo, M. E., Vacchi, M., Lorscheid, T., Stocchi, P., Gomez-Pujol, L., Harris, D. L., Casella, E., O'Leary, M. J., and Hearty, P. J.: The analysis of Last Interglacial (MIS 5e) relative sea-level indicators: Reconstructing sea-level in a warmer world, Earth Sci Rev, 159, 404–427, 2016b

Rovere, A., Ryan, D., Murray-Wallace, C., Simms, A., Vacchi, M., Dutton, A., Lorscheid, T., Chutcharavan, P., Brill, D., Bartz, M., Jankowski, N., Mueller, D., Cohen, K., and Gowan, E.: Descriptions of database fields for the World Atlas of Last Interglacial Shorelines (WALIS), https://doi.org/10.5281/zenodo.3961544, 2020.

Rovere, A., Ryan, D. D., Vacchi, M., Dutton, A., Simms, A. R., and Murray-Wallace, C. V.: The World Atlas of Last Interglacial Shorelines (version 1.0), Earth Syst Sci Data, 15, 1–23, https://doi.org/10.5194/essd-15-1-2023, 2023.

Ryan, W.B.F., Carbotte, S.M., Coplan, J.O., O'Hara, S., Melkonian, A., Arko, R., Weissel, R.A., Ferrini, V., Goodwillie, A., Nitsche, F., Bonczkowski, J. and Zemsky, R.: Global Multi-Resolution Topography synthesis, Geochem. Geophys. Geosyst., 10, Q03014, https://doi.org/10.1029/2008GC002332, 2009

Shennan, I.: Interpretation of Flandrian sea-level data from the Fenland, England, P. Geol. Assoc., 93, 53–63, 1982.

Shennan, I.: Flandrian sea-level changes in the Fenland. I: The geographical setting and evidence of relative sea-level changes, J. Quaternary Sci., 1, 119–153, 1986.

Shennan, I.: Holocene crustal movements and sea-level changes in Great Britain, J. Quaternary Sci., 4, 77–89, 1989.

Shennan, I.: Handbook of sea-level research, in: Handbook of Sea-Level Research, Wiley, 3–25, https://doi.org/10.1002/9781118452547.ch2, 2015.

https://doi.org/10.5194/essd-2026-153
Preprint. Discussion started: 22 June 2026

Shennan, I., Tooley, M. J., Davis, M. J., and Haggart, B. A.: Analysis and interpretation of Holocene sea-level data, Nature, 302, 404–406, 1983.

Talebian, M., & Jackson, J.: Offset on the Main Recent Fault of NW Iran and implications for the late Cenozoic tectonics of the Arabia–Eurasia collision zone. Geophysical Journal International, 150(2), 422–439, 2002

Thompson, S. B., & Creveling, J. R.: A global database of marine isotope substage 5a and 5c marine terraces and paleoshoreline indicators. Earth System Science Data, 13(7), 3467–3490, 2021

Woodroffe, C. D.: Late Quaternary sea-level highstands in the central and eastern Indian Ocean: A review. Global and Planetary Change, 47(2–4), 145–165, 2005

Woodroffe, C. D., McLean, R. F., Polach, H. A., & Thom, B. G.: Sea-level rise and coral reef development on the Cocos (Keeling) Islands. Coral Reefs, 10(4), 169–178, 1991